Jack Wilkie*, Paul D. Docherty, and Knut Möller

Developments in Modelling Bone Screwing

https://doi.org/10.1515/cdbme-2020-3029

Abstract: INTRODUCTION: A torque-rotation model of the bone-screwing process has been proposed. Identification of model parameters using recorded data could potentially be used to determine the material properties of bone. These properties can then be used to recommend tightening torques to avoid over or under-tightening of bone screws. This paper improves an existing model to formulate it in terms of material properties and remove some assumptions.
METHOD: The modelling methodology considers a critical torque, which is required to overcome friction and advance the screw into the bone. Below this torque the screw may rotate with elastic deformation of the bone tissue, and above this the screw moves relative to the bone, and the speed is governed by a speed-torque model of the operator's hand. The model is formulated in terms of elastic modulus, ultimite tensile strength, and frictional coefficient of the bone and the geometry of the screw and hole.
RESULTS: The model output shows the speed decreasing and torque increasing as the screw advances into the bone, due to increasing resistance. The general shape of the torque and speed follow the input effort. Compared with the existing model, this model removes the assumption of viscous friction, models the increase in friction as the screw advances into the bone, and is directly in terms of the bone material properties.
CONCLUSION: The model presented makes significant improvements on the existing model. However it is intended for use in parameter identification, which was not evaluated here. Further simulation and experimental validation is required to establish the accuracy and fitness of this model for identifying bone material properties.

Keywords: Orthopaedic surgery, self-tapping screw, smart screwdriver, bone modelling, parameter identification

1 Introduction

Correct torquing of bone screws is important to prevent failed implants. Implants may fail from loosening due to insufficient torque, or thread failure due to excessive torque[1]. Implant failure can damage the bone and surrounding tissue, or require risky revision surgery.

Currently, no known guidelines exist to recommended screw torques across patients and anatomical sites. Currently, surgeons tighten screws in an *ad-hoc* and presumably sub-optimal manner.

Heuristic approaches have previously been suggested in literature. Reynolds et al.[2] suggests a maximum torque as a multiple of the 'plateau torque' in a lag screw. Thomas et al.[3] recommends screwing should stop after detecting a spike in the derivative of torque with respect to time. Klingajay et al.[4] investigated simplistic model-based parameter identification for self-tapping screws in aluminium, but not bone. Klingajay et al.[4] used the model from Seneviratne et al.[5], which contributes some elements to the model proposed in this paper.

Wilkie et al.[1] proposed that a screwing process model can be used to identify bone material properties from recorded data. The model from Wilkie et al.[1] has opportunities for improvement, by formulating it in terms of material properties, and removing some assumptions. This paper further develops the model from Wilkie et al.[1]. There is potential for this model to allow a wider application to bone screwing that includes torque recommendations based on identified parameters in a model-based optimization.

2 Method

2.1 Overview

The modelling approach is similar to Wilkie et al.[1]. The screwing process is modelled using a critical torque. Below this torque, relative motion of the screw and bone is not possible, but the screw and bone tissue may rotate together due to elastic deformation in the bone. Above the critical torque, the screw advances at a speed governed by a model of input effort (analogous to a motor torque-speed curve).

The geometric constants are D_h [m], D_s [m], D_r [m], D_{re} [m], β [°], and p [m], as shown in Figure 1. Assuming $D_h > D_r$, D_r has no effect, and D_{re} can be determined from D_s, p, and β; therefore D_r and D_{re} are not used. The constant α [rad] is the angular length of the thread-cutting end of the screw. The bone material properties are ultimate tensile stress, σ_{uts} [Pa], elastic modulus E [Pa], Poisson's ratio, ν, and friction coefficient μ. The model variables are screw angular displacement, ϕ [rad], torque, T [Nm], and effort, ϵ.

***Corresponding author: Jack Wilkie,** Institute of Technical Medicine, Hochschule Furtwangen, Jakob-Kienzle-Straße 17, Schwenningen, Germany, e-mail: wij@hs-furtwangen.de
Paul D. Docherty, Center for Bioengineering, University of Canterbury, Christchurch, New Zealand
Knut Möller, Institute of Technical Medicine, Hochschule Furtwangen, Schwenningen, Germany

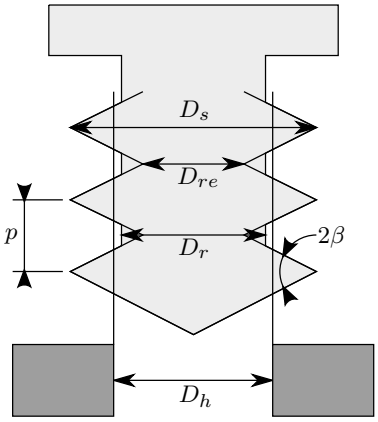

Fig. 1: Relationship of geometry constants to screw/hole shape

2.2 Critical Torque

Wilkie et al.[1] modelled critical torque as a constant value representing material strength. Here, a modified version of the model from Seneviratne et al.[5] was used. The critical torque (T_z [Nm]) is the sum of friction torque (T_{fz}) (assuming static and dynamic friction are equal), and the thread-cutting torque (T_{sz}). T_{fz} and T_{sz} are based on eq 26 and eq 10 in Seneviratne et al.[5], respectively. These formulae for T_{fz} and T_{sz} considered initial engagement and screw break-through, but this was removed here for simplicity; it is also assumed that $\sigma_{uts} = \sigma_f$. These modifications yield eq 1 and eq 2, and the sum in eq 3.

$$T_{fz} = 2\mu r_f K_{f0} \sigma_{uts} \cos\theta \left(\phi - a/2\right) \tag{1}$$

$$T_{sz} = r_s A_c \sigma_{uts} \cos\theta \tag{2}$$

$$T_z = T_{fz} + T_{sz} \tag{3}$$

The equations for r_f, r_s, K_{f0}, A_c, and θ from Seneviratne et al.[5] are given in equations 4, 5, 6, 7, and 8.

$$r_f = \left(D_h + D_s\right)/4 \tag{4}$$

$$r_s = \left(2D_h + 2D_s\right)/6 \tag{5}$$

$$K_{f0} = \tfrac{1}{2}(D_s - D_h)\sqrt{(1 + tan^2\beta)\left[\left(\tfrac{D_s+D_h}{4}\right)^2 + \left(\tfrac{p}{2\pi}\right)^2\right]} \tag{6}$$

$$A_c = \tan\beta \left(\frac{D_s - D_h}{2}\right)^2 \tag{7}$$

$$\theta = \tan^{-1}\frac{p}{\pi D_s} \tag{8}$$

Substituting eq 1 and eq 2 into eq 3, and factoring out geometric terms as per eq 9 and eq 10 gives T_z in terms of displacement and material properties in eq 11.

$$G_1 = r_s A_c \cos\theta \tag{9}$$

$$G_2 = 2 r_f K_{f0} \cos\theta \tag{10}$$

$$T_z = \sigma_{uts} G_1 + \mu \sigma_{uts} \left(\phi - \frac{\alpha}{2}\right) G_2 \tag{11}$$

2.3 Elastic Region

Below the critical torque, the screw can still be rotated due to elastic deformation in the bone, but there is no relative motion between the screw and the bone at the penetration site. The resisting torque provided by the elastic modulus of the bone will increase as the screw advances deeper into the material. The elastic behaviour was modelled by considering a flat disc of infinite diameter, with a torque τ applied in the centre; the disk thickness is equal to the screw depth z. The relationship between screw torque and angular displacement was examined by considering the infinitesimal element in Figure 2.

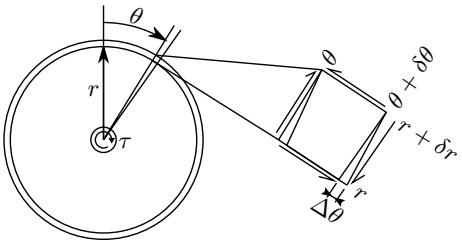

Fig. 2: Infinitesimal element under shear load

The torque τ applied at the centre will result in a shear force distributed around the cylindrical surface at radius r of $F = \tau/r$. The shear force on the element will be

$$\delta F = \frac{\tau \delta\theta}{2\pi r} \tag{12}$$

The area on the top surface of the element is $\delta A = r\delta\theta z$. Eq 14 is formed by substituting into the definition of shear strain, eq 13, and rearranging for $\Delta\theta = f(G)$.

$$G\left[= \frac{E}{2(1+\nu)}\right] = \frac{\delta F \delta r}{\delta A \Delta\theta} \tag{13}$$

$$\Delta\theta = \frac{\delta F \delta r}{\delta A G} = \frac{\tau \delta\theta \delta r}{2\pi r^2 \delta\theta z G} = \frac{\tau \delta r}{2\pi r^2 z G} \tag{14}$$

The screw rotation, θ_s, (assuming the screw is rigid) is found by integrating from $r = \infty$ to $r = r_s = (D_s + D_h)/4$:

$$\theta_s = \int_{r=\infty}^{(D_s+D_h)/4} \frac{\tau}{2r^2\pi z G} dr = -\tau \frac{2}{\pi z G (D_s + D_h)} \tag{15}$$

Using Hooke's law, $\tau = -k\theta$ or $k = -\tau/\theta$, substituting in eq 15, and converting linear to angular displacement with $z = \frac{p}{2\pi}\phi$, yields a conversion between k and G:

$$k = G\frac{\pi z (D_s + D_h)}{2} \tag{16}$$

So now while the $T < T_z$, the motion is modelled according to Hookes law, like in Wilkie et al.[1]:

$$\dot{\phi} = \frac{1}{k}\dot{T} \tag{17}$$

2.4 Motion Region

In Wilkie et al.[1], viscous friction was assumed for $T > T_z$ to regulate the screw insertion speed. It is instead assumed here, that the screwdriver operator will be able to produce the most torque at a rotational speed of zero, and maximum speed when no torque is exerted. The user will exert a varying effort, $\epsilon \in [0, 1]$, which will modulate this torque-speed curve. This effort will be the input variable to the model. For simplicity a linear curve is assumed, as shown in Figure 3, and mathematically in eq 18, where a and b are assumed to be known constants. a represents zero-load speed, and b represents the torque-speed gradient. For the elastic region, $\dot{\phi}$ is very small, so assuming $\dot{\phi} = 0$ gives eq 19.

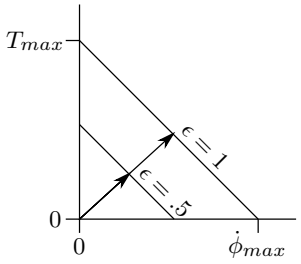

Fig. 3: Torque-speed model for hand operation of screwdriver

$$\dot{\phi} = a\epsilon - bT \tag{18}$$

$$T = \frac{a}{b}\epsilon \tag{19}$$

2.5 Final Model and Simulation

Using equation 18 for $T > T_z$ and 19 for $T < T_z$, and substituting in eq 17 and T_z, equations 20 and 21 are formed.

$$\dot{\phi} = \begin{cases} a\epsilon - bT_z(\phi) & a\epsilon \geq bT_z(\phi) \\ \frac{1}{bk}a\dot{\epsilon} & a\epsilon < bT_z(\phi) \end{cases} \tag{20}$$

$$T = \begin{cases} T_z(\phi) & a\epsilon \geq bT_z(\phi) \\ \frac{1}{b}a\epsilon & a\epsilon < bT_z(\phi) \end{cases} \tag{21}$$

This model was discretised and implemented in MATLAB. $\dot{\phi}$ was integrated to track ϕ. A repeating trapezoidal input was used to simulate the repetitive turning process a person would use. The initial condition $\phi = 2\pi$ avoided dividing by zero and simulated a partial pre-insertion of one turn. The model was simulated numerically at a rate of 10000 Hz to minimise errors from the discontinuity in $\dot{\phi}$ and T, with parameters summarised in Table 1. The outputs ϕ, $\dot{\phi}$ and T were tracked.

Tab. 1: Parameters for model simulation

Parameter	Value	Units	Notes/Source
E	300	MPa	Normal femoral head[6]
v	0.3		Generic estimate
σ_{uts}	3.5	MPa	Normal femoral head[6]
μ	0.4		Normal femoral head[7]
D_h	3.2	mm	[8]
D_s	6.5	mm	SYNTHES 216.060[8]
β	15	°	Estimate from photo[9]
p	2.75	mm	SYNTHES 216.060[8]
α	2π	rad	Estimate from photo[9]
a	4	$rad.s^{-1}$	Intuition
b	4	$\frac{rad.s^{-1}}{Nm}$	Intuition

3 Results

The input and outputs from the simulation are presented in Figure 4, with detail in Figure 5 showing elastic behaviour.

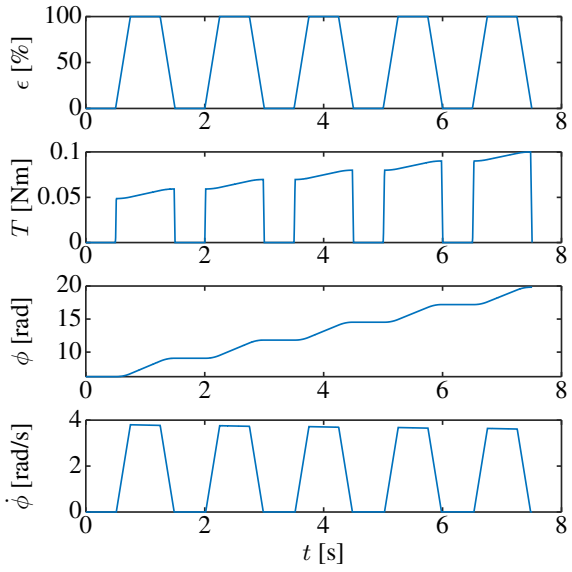

Fig. 4: Input and output variables of the model

4 Discussion

Figure 4 shows the basic behaviour of the model. The torque increases as the screw advances into the bone, due to increased frictional surface area. The speed follows an overall downward trend, as the required torque increases, resulting in a lower speed with the same effort.

Figure 5 shows the elastic behaviour of the model. As the material is stiff, and the torque is low, this elastic deformation is very small (about 0.00001 rad). In contrast, Wilkie et al.[1]

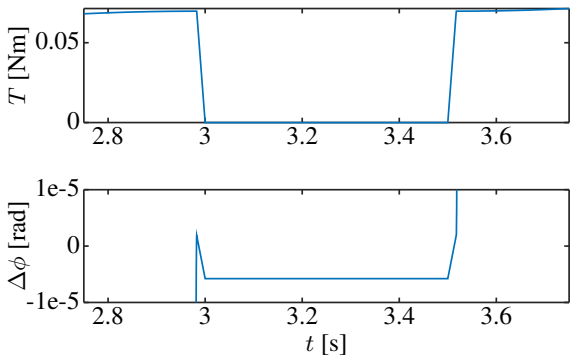

Fig. 5: Output zoomed to show elastic effect

used an arbitrary stiffness value as the relation to material properties was unknown, which had a much larger effect. The small size of this feature may make elasticity identification difficult. However, while the effect is sufficiently small to make identification difficult, this also implies that it may have a minimal affect in clinical application of the model. Further research is require to validate this assumption.

This model improves on Wilkie et al.[1] in a number of ways. It uses material properties for the parameters, whereas Wilkie et al.[1] used abstract parameters related to the material properties in an undefined manner. This model also removes the assumption of viscous friction; Chumakov[10] shows minimal effect of screwing speed on torque, suggesting that screwing does not exhibit viscous friction, but this used aluminium alloy which is not very strain-rate dependant[11]. In contrast, bone has shown significant strain rate dependence[12]. Experimentation is needed to check for viscous behaviour in bone during the screwing process. This model also considers friction changes as the screw advances into the bone, whereas Wilkie et al.[1] used a constant critical torque independent of depth.

The use of effort as an input is problematic. As effort cannot be measured like displacement or torque, it must be determined from the measured variables. As the relation between the variables is dependant on the unknown parameters, a heuristic method may be required.

This model also assumes bone is a continuous, isotropic, and homogeneous material. However bone has a complex, anisotropic composition. These assumptions will lead to imperfect predictions, but further study is required to determine if they are adequate. The discontinuous nature of bone (especially trabecular bone) may also introduce mechanical 'noise' into measurements, which is independent of sensor quality, and may require filtering.

This model has not been experimentally validated. Further work is needed to compare this model with experimental data and quantify its accuracy.

5 Conclusion

The model presented makes improvements on the model in Wilkie et al.[1]. However it will be used for parameter identification, and its fitness for this must still be established through further simulation and experimental validation.

Author Statement

Research funding: Partial support by grants "CiD" and "Digitalisation in the OR" from BMBF (Project numbers 13FH5E02IA and 13FH5I05IA). Conflict of interest: Authors state no conflict of interest. Ethical approval: The conducted research is not related to either human or animal use

References

[1] J Wilkie, P D Docherty, and K Möller. A simple screwing process model for bone material identification. *Proc. Automed.*, 1(1):038–038, 2020.

[2] K J Reynolds, A A Mohtar, T M Cleek, M K Ryan, and T C Hearn. Automated bone screw tightening to adaptive levels of stripping torque. *J. Orthop. Trauma*, 31(6):321–325, 2017.

[3] RL Thomas, K Bouazza-Marouf, and GJS Taylor. Automated surgical screwdriver: automated screw placement. *Proc. Inst. Mech. Eng. H*, 222(5):817–827, 2008.

[4] M Klingajay, L D Seneviratne, and K Althoefer. Parameter estimation during automated screw insertions. In *IEEE ICIT'02.*, volume 2, pages 1019–1024. IEEE, 2002.

[5] LD Seneviratne, FA Ngemoh, SWE Earles, and KA Althoefer. Theoretical modelling of the self-tapping screw fastening process. *Proc. Inst. Mech. Eng. C*, 215(2):135–154, 2001.

[6] B Li and R M Aspden. Composition and mechanical properties of cancellous bone from the femoral head of patients with osteoporosis or osteoarthritis. *J. Bone. Miner. Res.*, 12 (4):641–651, 1997.

[7] A Shirazi-Adl, M Dammak, and G Paiement. Experimental determination of friction characteristics at the trabecular bone/porous-coated metal interface in cementless implants. *J. Biomed. Mater. Res.*, 27(2):167–175, 1993.

[8] M Tsuji, M Crookshank, M Olsen, E H Schemitsch, and R Zdero. The biomechanical effect of artificial and human bone density on stopping and stripping torque during screw insertion. *J. Mech. Behav. Biomed.*, 22:146–156, 2013.

[9] West Coast Medical Resources, LLC. Synthes: 216.240. https://www.westcmr.com/synthes-216-240-216240. Accessed: 2020-04-01.

[10] R Chumakov. Optimal control of screwing speed in assembly with thread-forming screws. *Int. J. Adv. Manuf. Tech.*, 36(3-4): 395–400, 2008.

[11] Y Chen, AH Clausen, OS Hopperstad, and M Langseth. Stress–strain behaviour of aluminium alloys at a wide range of strain rates. *Int. J. Solids Struct.*, 46(21):3825–3835, 2009.

[12] F Linde, P Nørgaard, I Hvid, A Odgaard, and K Søballe. Mechanical properties of trabecular bone. dependency on strain rate. *J. Biomech.*, 24(9):803–809, 1991.